

# On the evolution process of two-component dark matter in the Sun

---

Chian-Shu Chen<sup>a</sup> and Yen-Hsun Lin<sup>b,1</sup>

<sup>a</sup>*Department of Physics, Tamkang University,  
New Taipei 251, Taiwan*

<sup>b</sup>*Department of Physics, National Cheng Kung University,  
Tainan 701, Taiwan*

*E-mail:* [chianshu@gmail.com](mailto:chianshu@gmail.com), [yenshun@phys.ncku.edu.tw](mailto:yenshun@phys.ncku.edu.tw)

**ABSTRACT:** We introduce dark matter (DM) evolution process in the Sun under a two-component DM (2DM) scenario. Both DM species  $\chi$  and  $\xi$  with masses heavier than 1 GeV are considered. In this picture, both species could be captured by the Sun through DM-nucleus scattering and DM self-scatterings, e.g.  $\chi\chi$  and  $\xi\xi$  collisions. In addition, the heterogeneous self-scattering due to  $\chi$  and  $\xi$  collision is essentially possible in any 2DM models. This new introduced scattering naturally weaves the evolution processes of the two DM species that was assumed to evolve independently. Moreover, the heterogeneous self-scattering enhances the number of DM being captured in the Sun mutually. This effect significantly exists in a broad range of DM mass spectrum. We have studied this phenomena and its implication for the solar-captured DM annihilation rate. It would be crucial to the DM indirect detection when the two masses are close. General formalism of the 2DM evolution in the Sun as well as its kinematics are studied.

**KEYWORDS:** dark matter evolution in the Sun, two-component dark matter, dark matter self-interaction

---

<sup>1</sup>Corresponding author.

---

## Contents

<b>1</b>	<b>Introduction</b>	<b>1</b>
<b>2</b>	<b>Remarks on the 2DM scenario</b>	<b>3</b>
2.1	Brief review of the 2DM models	3
2.2	Notation conventions and general assumptions	4
<b>3</b>	<b>General formalism of dark matter evolution in the Sun</b>	<b>5</b>
3.1	The 1DM evolution equation	5
3.2	The 2DM evolution equations	6
<b>4</b>	<b>Dark matter scattering rates</b>	<b>7</b>
4.1	The solar capture rate	7
4.2	The self-capture rate	7
4.3	The annihilation rate	9
4.4	The evaporation and self-ejection rates	9
<b>5</b>	<b>Numerical analysis: A model-independent treatment</b>	<b>10</b>
5.1	Number of dark matter particles in the Sun	10
5.2	Implication for the dark matter total annihilation rate in the Sun	12
<b>6</b>	<b>Summary</b>	<b>15</b>
<b>A</b>	<b>Derivations of the 2DM heterogeneous self-scattering rates</b>	<b>16</b>
A.1	The self-capture rate	16
A.2	The self-evaporation rate	18
A.3	The self-ejection rate	19

---

## 1 Introduction

Dark matter (DM) composes five times as prevalent as ordinary matter, yet its particle nature is still elusive. The essence of DM is often portrayed as Weakly Interacting Massive Particle (WIMP) with one specie. Experiments built to probe the interaction between the Standard Model (SM) particles and DM are running in progress [1–6]. Besides, terrestrial neutrino detectors [7–9] and satellite detectors [10–12] are designed to detect the SM particle fluxes from the annihilation of DM. Though much more stringent constraints on the DM properties have been set, primary implication for DM is generally from its gravitational influence. The understanding of DM is still in its budding stage.

Nevertheless, no strong evidence indicates that there exists only one-component DM in the dark sector (DS). DM with  $n$ -component ( $n$ DM) is also a plausible option. Each one

contributes relic abundance  $\Omega_\alpha h^2$  to the total relic abundance  $\Omega_{\text{DM}} h^2$  where  $\Omega_{\text{DM}} h^2 = \sum_\alpha \Omega_\alpha h^2 \approx 0.12$  [13] and  $h$  is the Hubble constant. Theoretical models on the two-component DM (2DM) scenario have been proposed recently [14–19]. Works regard the 2DM models on the direct and indirect searches can be also found in refs. [20–22] and references therein. In addition, cosmological  $N$ -body simulation incorporates 2DM that leads to the large scale structure which agrees the observation has been done recently [23].

In this work, we study the DM evolution in the Sun under the 2DM scenario with particle species  $\chi$  and  $\xi$ . Recent studies on solar captured 2DM are only a few, and, to our understanding, such studies consider the evolution of two species that are independent in the Sun. On the other hand, the collision between  $\chi$  and  $\xi$  does not account for the DM capture in the Sun. The collisions among DM particles are generally characterized as DM self-interactions. In the 1DM scenario, DM self-interaction [24–29] is addressed to alleviate the discrepancy between the collisionless  $N$ -body simulation and the observations. Such inconsistency arises from small-scale structure [30–39] could be resolved by imposing the constraint  $0.1 < \sigma_{\text{DM}}/m_{\text{DM}} < 10 \text{ cm}^2 \text{ g}^{-1}$ , where  $\sigma_{\text{DM}}$  and  $m_{\text{DM}}$  are DM self-interacting cross section and mass respectively. In addition, by incorporating baryonic effect, that the problem of diverse galactic rotation curves [40, 41] could be mitigated with the constraint  $3 < \sigma_{\text{DM}}/m_{\text{DM}} < 6 \text{ cm}^2 \text{ g}^{-1}$  [42–45].

The study of DM captured by the Sun has been investigated in refs. [46–51]. Updated calculation including the non-zero momentum transfer and implication for DM-electron capture are also indicated in ref. [52]. Our work is based on the earlier ones, and we further extend the framework to the 2DM scenario. The contribution to the capture rate from DM self-interaction denotes the self-capture in general. Furthermore, in the 2DM scenario, a plausible situation is that aside from  $\chi\chi$  and  $\xi\xi$  collisions, the self-interactions can also happen between  $\chi$  and  $\xi$ , the *heterogeneous* self-interaction. In this case,  $\chi\xi$  collision plays a role of heterogeneous self-capture. In the presence of heterogeneous self-interaction, extra coupling terms should be incorporated in the evolution equations. The evolution processes of  $\chi$  and of  $\xi$  cannot be treated separately. In our analysis, we found that the number of the sub-dominant DM specie is subject to a correction from the dominant DM specie. Nevertheless, the heterogeneous self-interaction not only increases the capture rate, it also responsible for the self-evaporation and self-ejection effects.

The general formalism to calculate the 2DM evolution in the Sun is given in this paper. Full expressions for the rates of DM-nucleus capture, evaporation and contributions from DM self-interaction including heterogeneous effects are presented. Although the framework shown here focuses on the 2DM scenario, it can be easily generalized to any  $n$ DM scenario. Unless subtle interaction is specified in the  $n$ DM case, e.g. 3-body scattering, the results provided in this paper are generally applied to any 2-body scattering with different masses. As a remark, when the 2DM scenario is invoked, co-annihilation could happen if the masses are nearly degenerate between  $\chi$  and  $\xi$  [53–55]. However, in the later analysis, we scan a broad range of DM mass spectrum. In most of the situation, the masses are not degenerate. Thus, the co-annihilation can be considered irrelevantly. Omitting it from our discussion is reasonable. Works in regard to co-annihilation and its implication for the solar-captured DM can be found in refs. [56, 57].

This paper is structured as follows. In section 2, we briefly introduce the 2DM scenario including notations and general assumptions in this work. In section 3, the evolution equations for  $\chi$  and  $\xi$  are given. Coupling terms from heterogeneous self-interaction are introduced in the equations. In section 4, we present all the rates of interaction. Physical implications are shown. In section 5, numerical results of the evolution equations are calculated along with the DM total annihilation rates for both species. If DM can annihilate to final state with SM particles, the DM total annihilation rate characterizes the intensity of such SM particle flux. Finally, we summarize in section 6. Mathematical derivations of the rates relative to the heterogeneous self-interaction are given in the appendix.

## 2 Remarks on the 2DM scenario

### 2.1 Brief review of the 2DM models

The 2DM models typically require two different discrete symmetries assigned to each DM to sustain their stability. However, simple extension of the SM group by a global discrete symmetry can be violated by gravity [58] or induce the cosmic defects that are not compatible with cosmological observations [59]. These problems can be evaded if one retains the wanted discrete symmetries by breaking a gauge group.

One of the simplest 2DM models is based on an Abelian  $U(1)_d$ , where  $d$  refers to hidden charge, and then assign some integer quantum numbers  $n_1$  and  $n_2$  to the hidden scalar fields  $\chi$  and  $\xi$  [60]. After  $\chi$  and  $\xi$  fields develop vacuum expectation values, the  $U(1)_d$  will break with the residual discrete symmetries  $Z_{n_1} \otimes Z_{n_2}$ . Examples are  $Z_2 \otimes Z'_2$  [16] or  $Z_2 \otimes Z_4$  [19]. As a result  $\chi$  and  $\xi$  can be both stable and will be the DM candidates. Other interesting models are the DM can be the multiplet of vector bosons of some hidden non-Abelian gauge groups [14, 15, 17, 18]. For example, a hidden  $SU(2)_d$  gauge group with a hidden fundamental representation of scalar field  $\phi$ ,

$$\mathcal{L}_d = -\frac{1}{4}F'^{a\mu\nu}F'_{\mu\nu} + (D_\mu\phi)^\dagger(D^\mu\phi) + V(\phi), \quad (2.1)$$

where  $a = 1, 2, 3$ ,  $F'^{a\mu\nu}$  is the hidden field strength,  $D^\mu\phi = \partial^\mu\phi - i\frac{g_d}{2}\tau^a \cdot A'^{a\mu}\phi$ ,  $g_d$  is the hidden coupling constant and  $A'^\mu$  is the hidden gauge field. After  $\phi$  developing a vacuum expectation value,  $SU(2)_d$  breaks and the corresponding hidden gauge bosons will become degenerate massive particles. In such case, a residual custodial  $SO(3)$  symmetry remains due to the fact of scalar field  $\phi$  being the fundamental representation. A  $Z_2 \otimes Z'_2$  discrete symmetry,

$$\begin{aligned} Z_2 : A'_\mu{}^1 &\rightarrow -A'_\mu{}^1, & A'_\mu{}^2 &\rightarrow -A'_\mu{}^2, \\ Z'_2 : A'_\mu{}^1 &\rightarrow -A'_\mu{}^1, & A'_\mu{}^3 &\rightarrow -A'_\mu{}^3, \end{aligned} \quad (2.2)$$

will apply to the hidden gauge bosons. Therefore,  $A'_\mu{}^a$  can be stable and DM candidates. One can extend the non-Abelian  $SU(2)_d$  to larger groups [17]. It is worth of mentioning that in such models the DM can interact with the SM sectors via Higgs portal,

$$\mathcal{L}_{\text{Higgs}} \supset -\mu^2 H^\dagger H + \lambda(H^\dagger H)^2 - \mu_\phi^2 \phi^\dagger \phi + \lambda_\phi(\phi^\dagger \phi)^2 + \lambda_{H\phi} \phi^\dagger \phi H^\dagger H. \quad (2.3)$$

or gauge boson kinetic mixing,

$$\mathcal{L}_{\text{gauge}} \supset \varepsilon B_{\mu\nu} X^{\mu\nu} \quad (2.4)$$

where  $B_{\mu\nu}$  and  $X_{\mu\nu}$  are the field strength of  $U(1)_Y$  and  $U(1)_d$  respectively. Therefore the DM annihilation final states are SM particles or new scalars if it is kinematically allowed. These DM particles behave as thermal WIMPs and can retain the observed DM relic abundance. Interesting phenomena provided by these DM particles, e.g. excess cosmic rays, direct search, cosmology and collider physics, can be found in refs. [14, 15, 17, 18, 61–67] and references therein.

## 2.2 Notation conventions and general assumptions

Suppose the two DM species  $\chi$  and  $\xi$  only differ in mass such that  $m_\chi \neq m_\xi$  in general. The corresponding relic abundances are  $\Omega_\alpha h^2$  where  $\alpha = \chi$  and  $\xi$ . Assuming DM as the thermal relic and its total abundance  $\Omega_{\text{DM}} h^2$  is made up of  $\Omega_\chi h^2$  and  $\Omega_\xi h^2$ , e.g.  $\Omega_{\text{DM}} h^2 = \Omega_\chi h^2 + \Omega_\xi h^2$ . Ratio of the two relic abundances can be defined by

$$r_\rho = \frac{\Omega_\xi}{\Omega_\chi}. \quad (2.5)$$

If the annihilation is dominated by  $s$ -wave process at freeze-out epoch, we have the relic abundance inversely proportional to its thermal relic annihilation cross section  $\langle \sigma v \rangle_0$  that is given by [46]

$$\Omega_\alpha h^2 \propto \frac{1}{\langle \sigma_\alpha v \rangle_0} \quad (2.6)$$

which is mass-independent up to logarithmic corrections. Hence, we can express the annihilation cross sections by  $r_\rho$ :

$$r_\rho = \frac{\langle \sigma_\chi v \rangle_0}{\langle \sigma_\xi v \rangle_0}. \quad (2.7)$$

Therefore, with eqs. (2.6) and (2.7), we can further define an *effective* annihilation cross section  $\langle \sigma_{\text{eff}} v \rangle_0$  for  $\Omega_{\text{DM}} h^2$  by

$$\Omega_{\text{DM}} h^2 = \Omega_\chi h^2 + \Omega_\xi h^2 \propto \frac{1 + r_\rho}{\langle \sigma_\chi v \rangle_0} \equiv \frac{1}{\langle \sigma_{\text{eff}} v \rangle_0}. \quad (2.8)$$

To produce thermal relic abundance  $\Omega_{\text{DM}} h^2 \approx 0.12$  [13], it is reasonable to assume  $\langle \sigma_{\text{eff}} v \rangle_0 \approx 3 \times 10^{-26} \text{ cm}^3 \text{ s}^{-1}$ .

In addition, the number of DM particles captured by the Sun is relevant to the local DM density  $\rho_{\text{DM}}$  around our solar neighborhood. Thus, the relation

$$\rho_{\text{DM}} = 0.3 \text{ GeV cm}^{-3} = \rho_\chi + \rho_\xi \quad (2.9)$$

that should hold. Without loss of generality, we let  $\rho_\alpha \propto \Omega_\alpha h^2$ , thus  $r_\rho = \rho_\xi / \rho_\chi$ . We can rewrite the above identity as

$$\rho_{\text{DM}} = \rho_\chi (1 + r_\rho) = 0.3 \text{ GeV cm}^{-3} \quad (2.10)$$

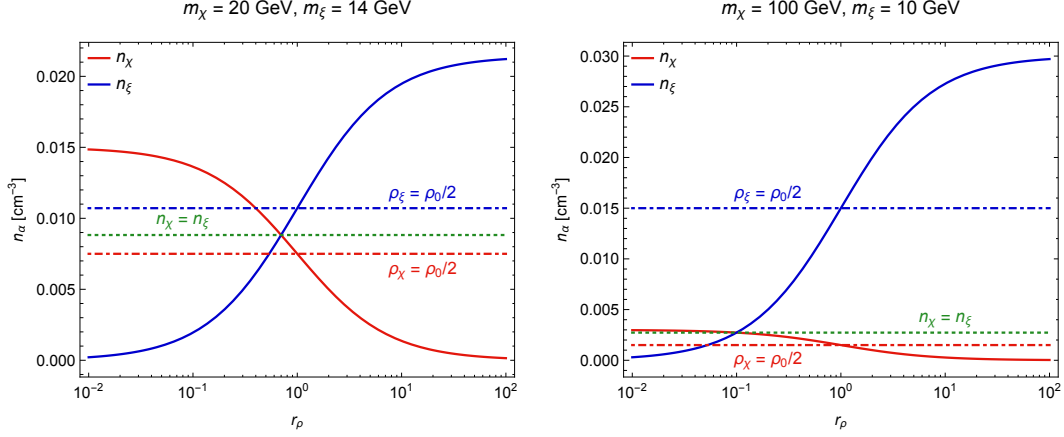


**Figure 1.** Local DM number density  $n_\alpha$  vs.  $r_\rho$ .  $\rho_{\text{DM}} = 0.3 \text{ GeV cm}^{-3}$  is the local DM density near the solar neighborhood. A similar result can be also found in the figure 1 of ref. [22].

and the local DM number density  $n_\alpha = \rho_\alpha/m_\alpha$  is plotted in figure 1 versus  $r_\rho$ . A similar plot can be found in the figure 1 of ref. [22] as well. When  $r_\rho = 1$ , the DM with lighter mass has the higher number density. On the other hand, the number densities happen to be equal when  $r_\rho = m_\xi/m_\chi$ . In the later analysis, we assume the validations of eqs. (2.7), (2.8) and (2.10) pass to the present day. Once  $r_\rho$  is assigned,  $\langle\sigma_\alpha v\rangle$  and  $\rho_\alpha$  are specified consequently.

### 3 General formalism of dark matter evolution in the Sun

#### 3.1 The 1DM evolution equation

When the Sun sweeps the DM halo, DM particles are attracted by the solar gravity. The subsequent scatterings with the solar nuclei and other DM particles already trapped in the Sun could happen. DM particles can be captured by the Sun when its final velocity is smaller than the escape velocity of the Sun after scattering. Alternatively, DM particles trapped inside the Sun will be kicked out if its final velocity after the scattering with the nuclei is larger than the escape velocity. The inclusion of DM self-interaction will also have effects on the capture and evaporation of DM particles in the Sun. Incorporating all these effects, the general equation describes the DM evolution process is given by

$$\frac{dN_{\text{DM}}}{dt} = C_c + (C_s - C_e)N_{\text{DM}} - (C_a + C_{se})N_{\text{DM}}^2 \quad (3.1)$$

where  $N_{\text{DM}}$  is the DM number in the Sun,  $C_c$  the rate at which DM is captured by the solar nuclei [47–49, 52],  $C_s$  the self-capture rate at which DM is captured due to scattering with other trapped DM inside the Sun [68],  $C_e$  the evaporation rate due to DM-nucleus scattering [69],  $C_a$  the annihilation and  $C_{se}$  the self-evaporation rate that caused by DM-DM scattering [70].

However, recent study shows unless DM mass  $m_{\text{DM}} \lesssim 4 \text{ GeV}$ , the evaporation effect is much inefficient even with the inclusion of  $C_{se}$  [70]. Thus, in the absence of evaporations, eq. (3.1) reads

$$\frac{dN_{\text{DM}}}{dt} = C_c + C_s N_{\text{DM}} - C_a N_{\text{DM}}^2 \quad (3.2)$$

along with an analytical solution

$$N_{\text{DM}} = \frac{C_c \tanh(t/\tau)}{\tau^{-1} - C_s \tanh(t/\tau)/2}, \quad (3.3)$$

where  $\tau = 1/\sqrt{C_c C_a + C_s^2/4}$  is the equilibrium timescale. When  $t \gg \tau$ ,  $dN_{\text{DM}}/dt = 0$ .

### 3.2 The 2DM evolution equations

On the other hand, eq. (3.1) only characterizes 1DM scenario. Once the second DM specie is included, additional evolution equation should be added. In this scenario, the self-interactions are not only due to  $\chi\chi$  and  $\xi\xi$  scatterings as well as  $\chi\xi$  scattering. Thus, the evolution process is determined by

$$\frac{dN_\chi}{dt} = C_c^\chi + (C_s^\chi - C_e^\chi)N_\chi + (C_s^{\chi \rightarrow \xi} - C_{se}^{\chi \rightarrow \xi}N_\chi)N_\xi - (C_a^\chi + C_{se}^\chi)N_\chi^2, \quad (3.4a)$$

$$\frac{dN_\xi}{dt} = C_c^\xi + (C_s^\xi - C_e^\xi)N_\xi + (C_s^{\xi \rightarrow \chi} - C_{se}^{\xi \rightarrow \chi}N_\xi)N_\chi - (C_a^\xi + C_{se}^\xi)N_\xi^2. \quad (3.4b)$$

The above equations are modified from eq. (3.1). Four additional coefficients are introduced.  $C_s^{\chi(\xi) \rightarrow \xi(\chi)}$  denote the heterogeneous self-capture rates due to halo  $\chi(\xi)$  scatters with trapped  $\xi(\chi)$  in the Sun.  $C_{se}^{\chi(\xi) \rightarrow \xi(\chi)}$  denote the heterogeneous self-evaporation rates due to the  $\chi(\xi)$  scatters with  $\xi(\chi)$  in the Sun. The rest are  $C_c^\alpha$  the solar captures,  $C_s^\alpha$  the self-capture rates,  $C_e^\alpha$  the evaporation rates,  $C_{se}^\alpha$  the self-evaporation rates and  $C_a^\alpha$  the annihilation rates as those in the 1DM case.

Both eqs. (3.4a) and (3.4b) correlate together through the terms subject to  $N_\xi$  in  $dN_\chi/dt$  and  $N_\chi$  in  $dN_\xi/dt$ . The DM numbers of  $\chi$  and of  $\xi$  in the Sun are mutually dependent. Without correlation terms, the evolution processes for both DM species are decoupled. Generally, evaporation is inefficient unless the DM mass is light enough, typically when  $m_\alpha^{\text{ev}} \lesssim 4 \text{ GeV}$ . Even including the extra contribution  $C_{se}^{\chi(\xi) \rightarrow \xi(\chi)}$ , we have numerically justified that this effect does not change the  $m_\alpha^{\text{ev}}$  dramatically. Thus, when  $m_\alpha > 4 \text{ GeV}$ , we can safely ignore the evaporation from eqs. (3.4a) and (3.4b). Therefore,

$$\frac{dN_\chi}{dt} = C_c^\chi + C_s^\chi N_\chi + C_s^{\chi \rightarrow \xi} N_\xi - C_a^\chi N_\chi^2, \quad (3.5a)$$

$$\frac{dN_\xi}{dt} = C_c^\xi + C_s^\xi N_\xi + C_s^{\xi \rightarrow \chi} N_\chi - C_a^\xi N_\xi^2. \quad (3.5b)$$

But in the later numerical calculations, we will always use the general expressions eqs. (3.4a) and (3.4b). Note that the evolution equations have no analytical expressions on  $N_\alpha$  and  $\tau$  in the 2DM scenario. However, approximated expressions can be obtained in certain situations. It will be discussed in section 5.

## 4 Dark matter scattering rates

### 4.1 The solar capture rate

The solar capture rate due to DM-nucleus scattering can be numerically approximated as [55, 71]

$$C_c^{\text{SI}} \simeq 4.1 \times 10^{24} \text{ s}^{-1} \left( \frac{\rho_\alpha}{\text{GeV cm}} \right) \left( \frac{270 \text{ km s}^{-1}}{\bar{v}} \right)^3 \left( \frac{\sigma_{\text{H}}^{\text{SI}} + 0.175 \sigma_{\text{He}}^{\text{SI}}}{10^{-6} \text{ pb}} \right) \left( \frac{\text{GeV}}{m_\alpha} \right)^2 \quad (4.1)$$

for spin-independent (SI) case and

$$C_c^{\text{SD}} \simeq 1.12 \times 10^{25} \text{ s}^{-1} \left( \frac{\rho_\alpha}{\text{GeV cm}} \right) \left( \frac{270 \text{ km s}^{-1}}{\bar{v}} \right)^3 \left( \frac{\sigma_{\text{H}}^{\text{SD}}}{10^{-6} \text{ pb}} \right) \left( \frac{\text{GeV}}{m_\alpha} \right)^2 \quad (4.2)$$

for spin-dependent (SD) case.  $\rho_\alpha$  is the DM local density and  $\bar{v} = 270 \text{ km s}^{-1}$  the DM velocity dispersion.  $\sigma_{\text{H,He}}^{\text{SI,SD}}$  is the DM-nucleus scattering cross section for hydrogen or helium. Taking proton mass  $m_p$  is close to neutron mass  $m_n$ . The DM-nucleus cross section  $\sigma_A$  at which interaction is undergoing that is related to DM-nucleon cross section  $\sigma_{\alpha p}$  by

$$\sigma_A^{\text{SI}} = A^2 \left( \frac{m_A}{m_p} \right)^2 \left( \frac{m_\alpha + m_p}{m_\alpha + m_A} \right)^2 \sigma_{\alpha p}^{\text{SI}} \quad (4.3)$$

for SI interaction and

$$\sigma_A^{\text{SD}} = A^2 \left( \frac{m_\alpha + m_p}{m_\alpha + m_A} \right)^2 \frac{4(J+1)}{3J} |\langle S_p \rangle + \langle S_n \rangle|^2 \sigma_{\alpha p}^{\text{SD}} \quad (4.4)$$

for SD interaction, where  $A$  is the atomic number,  $m_A$  the corresponding nucleus mass,  $J$  the total angular momentum of the nucleus and  $\langle S_p \rangle$  and  $\langle S_n \rangle$  the spin expectation values of proton and of neutron averaged over the entire nucleus [72–77]. To apply the above results, we have assumed  $\chi$  and  $\xi$  obey the same Maxwell-Boltzman velocity distribution. The effect of uncertainties in velocity distributions to the capture rate is minor [78]. We note that  $\sigma_{\alpha p}$  is a model-dependent parameter in general.

In addition, following earlier work [71], refined calculation on solar capture rate including the contributions from elements beyond hydrogen and helium can be found in refs. [49, 52]. In ref. [52], constant scattering cross section as well as velocity-dependent and transfer-momentum-dependent cases are fully considered. We adopt the numerical procedure in ref. [52] to calculate  $C_c$  in the 2DM scenario.

### 4.2 The self-capture rate

The self-capture happens when the halo DM particles scatter off the DM particles that are already trapped inside the Sun. Starting with halo  $\chi$  particle captured by the trapped  $\xi$  particle in the Sun. Therefore, the coefficient of heterogeneous self-capture rate can be expressed as

$$C_s^{\chi \rightarrow \xi} = \frac{\int 4\pi r^2 (dC_s^{\chi \rightarrow \xi} / dV) dr}{\int 4\pi r^2 n_\xi(r) dr} \quad (4.5)$$



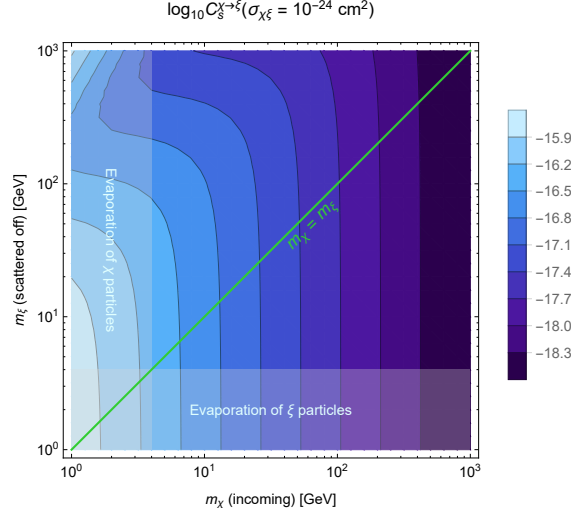


**Figure 2.** Self-capture coefficient  $C_s^{\chi \rightarrow \xi}$  and  $\sigma_{\chi\xi} = 10^{-24} \text{ cm}^2$ . The green line denotes the self-capture as a result of the same DM specie. White shaded region is the evaporation dominant region. Null capture happens here.

where  $dC_s^{\chi \rightarrow \xi}/dV$  is the heterogeneous self-capture rate in the Sun within a given shell. It is determined by  $m_\chi$ ,  $m_\xi$  and  $\sigma_{\chi\xi}$  where  $\sigma_{\chi\xi}$  is the heterogeneous self-scattering cross section. The analytical form of  $dC_s^{\chi \rightarrow \xi}/dV$  is given in eq. (A.11). Assuming the heat exchanges among DM particles are very efficient after capture. They will quickly reach the thermal equilibrium temperature  $T_\alpha = T$ . Therefore,  $n_\alpha(r) = n_\alpha^0 e^{-m_\alpha \phi(r)/T}$  where  $n_\alpha^0$  is the DM number density in the solar core,  $\phi(r) = \int_0^r GM(r')/r'^2 dr'$  and  $M(r')$  the solar mass enclosed by radius  $r'$ . The case for halo  $\xi$  particle captured by trapped  $\chi$  particle is essentially the same. Simply swaps  $\chi$  and  $\xi$  and replace all  $\chi$ 's parameters by  $\xi$ 's.

The expression given in eq. (4.5) is generally for  $m_\chi \neq m_\xi$ . Nevertheless, if the capture is due to the same DM specie, e.g.  $\chi\chi$  or  $\xi\xi$  scatterings, it is done by letting  $m_\chi = m_\xi$  and denotes as  $C_s^\alpha$ . Such that we have a rather simple analytical expression [68]:

$$C_s^\alpha = \sqrt{\frac{3}{2}} n_\alpha \sigma_\alpha v_{\text{esc}}(R_\odot) \frac{v_{\text{esc}}(R_\odot)}{\bar{v}} \langle \hat{\phi}_\alpha \rangle \frac{\text{erf}(\eta)}{\eta} \quad (4.6)$$

where  $\sigma_\alpha$  is the self-scattering cross section,  $\langle \hat{\phi}_\alpha \rangle \simeq 5.1$  [47] a dimensionless average solar potential experienced by the captured DM within the Sun and  $v_{\text{esc}}(R_\odot) \approx 632 \text{ km s}^{-1}$  the Sun's escape velocity at surface. We will characterize  $\sigma_\alpha$  by

$$\sigma_\alpha/m_\alpha \approx 3 \text{ cm}^2 \text{ g}^{-1} \quad (4.7)$$

in the later numerical analysis. Such relation appears to alleviate the diversity of galactic rotation curve in the presence of baryonic effect as well as small-scale structure problems [42]. Plot for  $C_s^{\chi \rightarrow \xi}$  in the  $m_\chi - m_\xi$  plane is shown in figure 2.

### 4.3 The annihilation rate

When more and more DM particles accumulate in the Sun, the rate of annihilation becomes stronger. The coefficient of annihilation rate is expressed as

$$C_a^\alpha = \langle \sigma_\alpha v \rangle \frac{\int_0^{R_\odot} n_\alpha^2(r) 4\pi r^2 dr}{[\int_0^{R_\odot} n_\alpha(r) 4\pi r^2 dr]^2} \quad (4.8)$$

where  $\langle \sigma v \rangle$  is the DM annihilation cross section. An approximation for  $C_a^\alpha$  is given by [46]

$$C_a^\alpha = \langle \sigma_\alpha v \rangle \frac{V_2}{V_1^2} \quad (4.9a)$$

where

$$V_j \approx 6.8 \times 10^{28} \text{ cm}^3 \left( \frac{T}{T_\odot} \right)^{3/2} \left( \frac{10 \text{ GeV}}{jm_\alpha} \right)^{3/2}, \quad j = 1, 2; \quad (4.9b)$$

is the DM effective volume and  $T_\odot = 1.54 \times 10^7 \text{ K}$  the solar core temperature. Essentially, the DM temperature  $T$  is not necessary the same as the solar temperature  $T_\odot$  [52, 79] and depends on  $m_\alpha$ . But the temperature deviation from  $T_\odot$  is generally small and has little impact on the final number of DM particles in the Sun. It is reasonable to impose  $T = T_\odot$  in our later discussion.

### 4.4 The evaporation and self-ejection rates

In the Sun, after the collision happens between two particles, if one gets velocity larger than the escape velocity  $v_{\text{esc}}$ , it won't be captured. This effect is called evaporation. When the evaporation is caused by DM-nucleus scattering, an approximation is given in ref. [80]

$$C_e^\alpha \simeq \frac{8}{\pi^2} \sqrt{\frac{2m_\alpha}{\pi T}} \frac{v_{\text{esc}}^2(0)}{\bar{r}^3} e^{-m_\alpha v_{\text{esc}}^2(0)/2T} \Sigma_{\text{evap}}, \quad (4.10)$$

where  $v_{\text{esc}}(0) = 1366 \text{ km s}^{-1}$  is the escape velocity at solar core,  $\bar{r}$  the mean DM distance from the solar center. The quantity  $\Sigma_{\text{evap}}$  is a factor that relates to the DM-nucleus scattering cross section [80]. The expression  $C_e^\alpha$  is valid when  $m_\alpha/m_A > 1$ . In our calculation, we modified the numerical procedure done in ref. [52] for the 2DM scenario.

Likewise, evaporation can happen as a result of  $\chi$  particle scattering off  $\xi$  particle in the Sun and vice versa. Hence we obtain coefficient of heterogeneous self-evaporation is given by

$$C_{se}^{\chi \rightarrow \xi} = \frac{\int 4\pi r^2 (dC_{se}^{\chi \rightarrow \xi}/dV) dr}{(\int 4\pi r^2 n_\chi(r) dr)(\int 4\pi r^2 n_\xi(r) dr)} \quad (4.11)$$

where  $dC_{se}^{\chi \rightarrow \xi}/dV$  is the heterogeneous self-evaporation in the Sun within a given shell. It is a function of  $m_\chi$ ,  $m_\xi$  and  $\sigma_{\chi\xi}$  and its analytical form is expressed in eq. (A.18). If the self-evaporation is due to either  $\chi$  or  $\xi$  itself, simply let  $m_\chi = m_\xi$  with additional factor of 1/2 to avoid over counting. The plot of  $C_{se}^{\chi \rightarrow \xi}$  against  $m_\chi$  is given in figure 3.

In addition, if a DM particle in the halo transports enough kinetic energy to the trapped DM particle in the Sun and leads to the trapped DM particle being ejected to the interstellar space. This is called the (heterogeneous) self-ejection. Numerical calculations

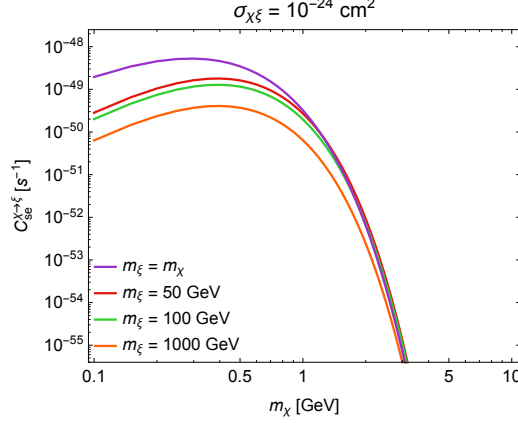


**Figure 3.** The self-evaporation coefficient  $C_{se}^{\chi \rightarrow \xi}$ . It is easily seen from the plot that when  $m_{\chi} > 4$  GeV, the effect is small enough to ignore it.

show the self-ejection effect is always small, compared to the self-capture one. Thus, we can ignore this effect safely from the calculation. Discussion on self-ejection rate is presented in the appendix A.3.

## 5 Numerical analysis: A model-independent treatment

### 5.1 Number of dark matter particles in the Sun

In the following analysis, when  $r_{\rho}$  is assigned, the annihilation cross section  $\langle \sigma_{\alpha} v \rangle$  and  $\rho_{\alpha}$  can be specified through eqs. (2.8) and (2.10). Thus, thermal relic abundance  $\Omega_{\text{DM}} h^2 \approx 0.12$  and  $\rho_{\text{DM}} = 0.3 \text{ GeV cm}^{-3}$  would be satisfied automatically. In the later numerical analysis, we have taken that  $\sigma_{\alpha p}^{\text{SI}} = 10^{-46} \text{ cm}^2$  as a benchmark value for SI case. It is slightly smaller than the most stringent value of LUX when the DM mass is roughly around 30 GeV [3]. For SD case,  $\sigma_{\alpha p}^{\text{SD}} = 10^{-42} \text{ cm}^2$  that is chosen not to violate the results from Super-K [8], PICO-60 [4] and IceCube [9]. The self-scattering cross section  $\sigma_{\alpha}$  is indicated from eq. (4.7) and we set  $\sigma_{\chi\xi} = 10^{-23} \text{ cm}^2$  and  $10^{-24} \text{ cm}^2$  as the benchmark values. These two values are within  $0.1 \text{ cm}^2 \text{ g}^{-1} \leq \sigma_{\text{DM}}/m_{\text{DM}} \leq 10 \text{ cm}^2 \text{ g}^{-1}$  in the whole interested mass range. The value of  $\sigma_{\chi\xi}$  tells us how  $\chi$  and  $\xi$  intertwine during the evolution. The number of DM particles in the Sun,  $N_{\alpha}$ , is plotted in figure 4 versus time  $t$ . We have fixed  $m_{\chi}$  at 1000 GeV and calculated with  $m_{\xi} = 100$  GeV and 10 GeV. The case for  $\sigma_{\chi\xi} = 0$  is labeled as *decoupled* for comparison.

Number of DM in the Sun,  $N_{\alpha}$ , is proportional to its local number density  $n_{\alpha} = \rho_{\alpha}/m_{\alpha}$  when reaches equilibrium stage. Suppose  $r_{\rho} = 1$  and  $m_{\chi} \gg m_{\xi}$ . We have  $n_{\chi} \ll n_{\xi}$ . Thus,  $\chi$  affects little on the evolution of  $\xi$ . Hence, in the equilibrium stage, we could drop  $C_s^{\xi \rightarrow \chi} N_{\chi}^{\text{eq}}$

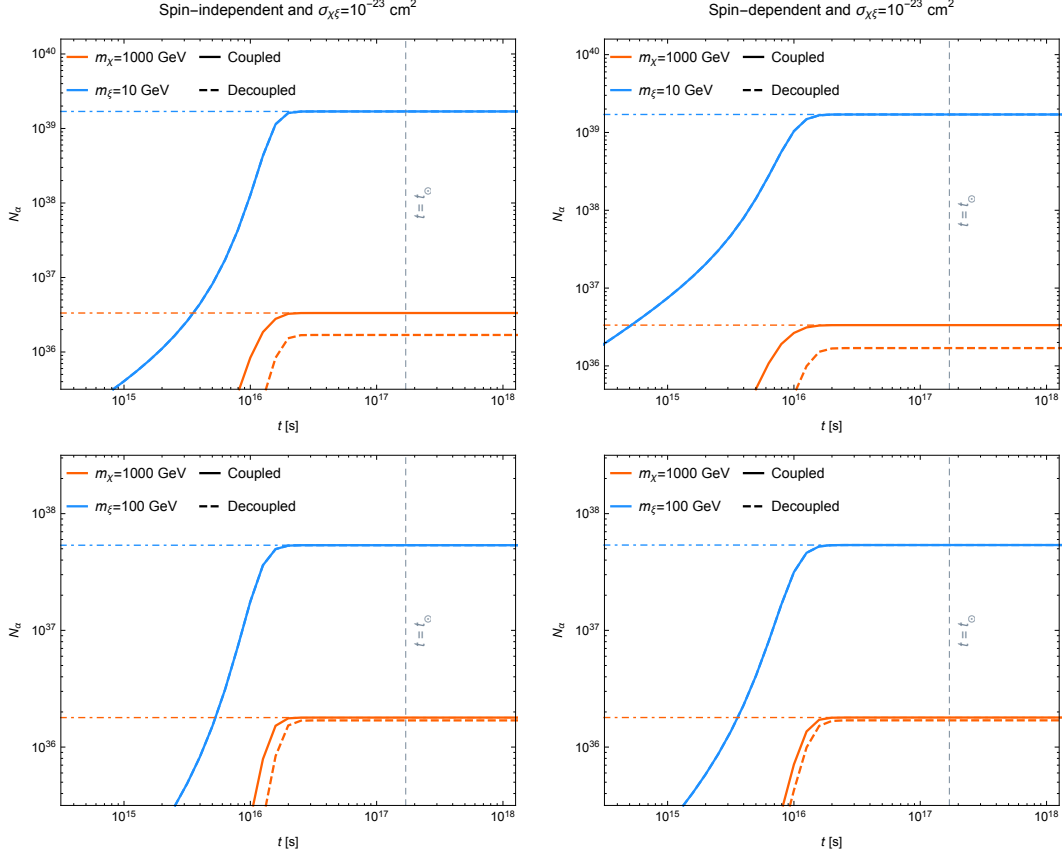


**Figure 4.** Evolution of DM numbers in the Sun with  $r_\rho = 1$ . We fixed  $m_\chi = 1000$  GeV and from top to down  $m_\xi = 10$  GeV and 100 GeV respectively. *Left panels:* spin-independent. *Right panels:* spin-dependent. Gray dashed line indicates current solar age  $t = t_\odot \approx 1.7 \times 10^{17}$  s. Dot-dashed lines in each figure represent the  $N_\alpha^{\text{eq}}$  approximations calculated from eqs. (5.1a) and (5.1b).

in eq. (3.5b). In this way, simple expressions for  $N_\chi^{\text{eq}}$  and  $N_\xi^{\text{eq}}$  can be given by

$$N_\chi^{\text{eq}} = \frac{C_s^\chi}{C_a^\chi} \left( \frac{1}{2} + \sqrt{\frac{1}{4} + R_\chi} \right) \quad (5.1a)$$

$$N_\xi^{\text{eq}} = \frac{C_s^\xi}{C_a^\xi} \left( \frac{1}{2} + \sqrt{\frac{1}{4} + R_\xi} \right) \quad (5.1b)$$

where

$$R_\chi = \frac{C_a^\chi (C_c^\chi + C_s^{\chi \rightarrow \xi} N_\xi^{\text{eq}})}{(C_s^\chi)^2} \quad \text{and} \quad R_\xi = \frac{C_a^\xi C_c^\xi}{(C_s^\xi)^2} \quad (5.1c)$$

are the correction factors due to the (heterogeneous) self-captures. We have verified eqs. (5.1a) and (5.1b) and they agree with numerical solutions of eqs. (3.5a) and (3.5b) very well after reaching the equilibrium state. See dot-dashed lines in figure 4. When  $n_\xi \gg n_\chi$ ,  $\xi$  evolves solely in the Sun. But  $N_\chi^{\text{eq}}$  is subject to a correction that is proportional to  $\sigma_{\chi\xi} N_\xi^{\text{eq}}$ . In addition, we take eq. (4.7) as the benchmark value of  $\sigma_\alpha$ . It results in a very strong self-interacting effect. Therefore, the DM numbers in the equilibrium state,  $N_\alpha^{\text{eq}}$ ,

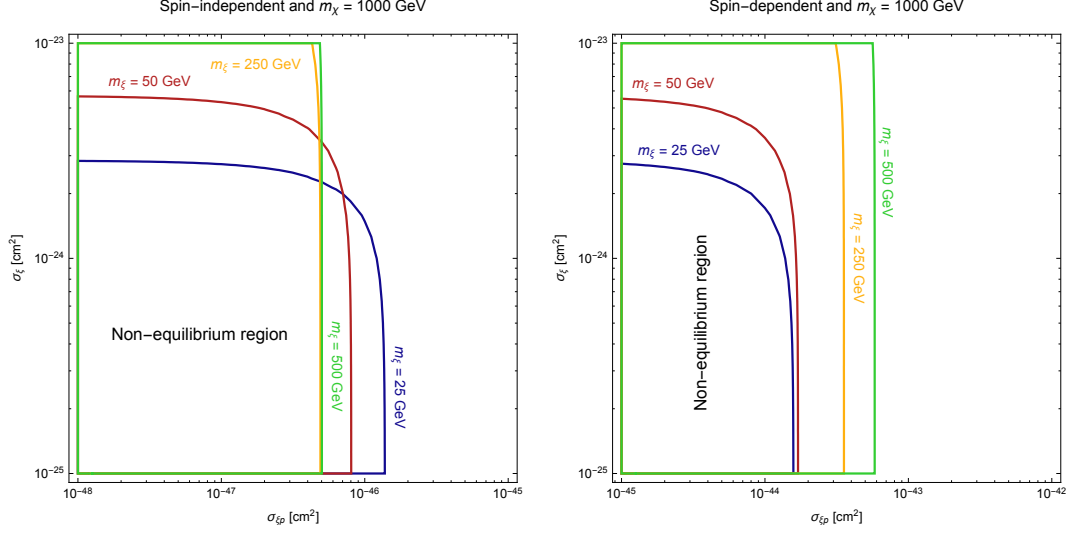


**Figure 5.** Equilibrium region for  $m_\xi = 25$  GeV (dark blue), 50 GeV (dark red), 250 GeV (light orange) and 500 GeV (lime green). *Left:* SI case. *Right:* SD case. Region enclosed by each contour represents non-equilibrium,  $t_\odot/\tau < 1$ , at current epoch. It is assumed that  $r_\rho = 1$ . In this choice of  $m_\chi$  and  $m_\xi$ , the equilibrium timescale is always determined by  $\xi$  solely. Thus, the effect of  $\sigma_{\chi\xi}$  can be omitted. See main text for detail.

is mostly determined by the interactions in the DS. This agrees with the conclusion in ref. [79] for 1DM case.

On the other hand, equilibrium must achieve simultaneously for both DM species. When  $n_\xi \gg n_\chi$ , the equilibrium timescale can be determined by  $\xi$  solely. It is given by  $\tau_\xi = 1/\sqrt{C_c^\xi C_a^\xi + (C_s^\xi)^2/4}$ . Therefore, the role plays by  $\sigma_{\chi\xi}$  that is insignificant and can be omitted. In figure 5, equilibrium region for a given  $m_\xi$  is indicated by its corresponding color contour. The place enclosed by the contour indicates  $t_\odot/\tau < 1$  as well as the non-equilibrium region.

Note that when  $m_\chi = m_\xi$ ,  $C_s^{\chi \rightarrow \xi} = C_s^\chi$  and  $C_s^{\xi \rightarrow \chi} = C_s^\xi$ . The evolution equations eqs. (3.4a) and (3.4b) are degenerate. It can be considered as an 1DM scenario.

## 5.2 Implication for the dark matter total annihilation rate in the Sun

When an appreciated amount of DM particles accumulate in the solar core, the total annihilation rate<sup>1</sup> as a result of these particles is given by

$$\Gamma_\alpha = \frac{1}{2} C_a^\alpha N_\alpha^2. \quad (5.2)$$

<sup>1</sup>The adjective *total* does not imply summing over  $\alpha$  but sum over all the DM number either from  $\chi$  or  $\xi$  in the Sun.

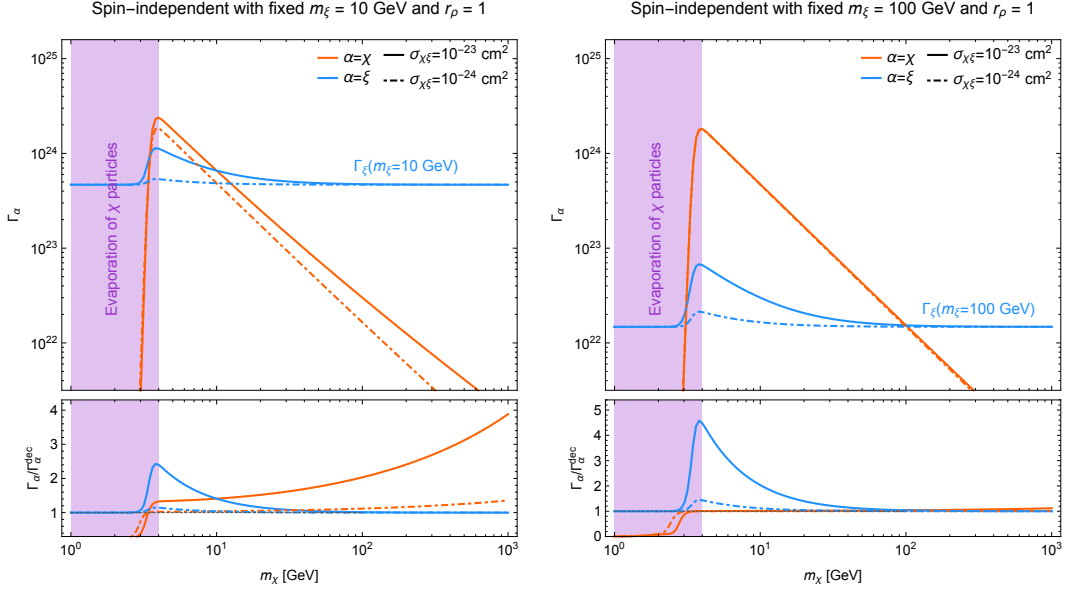


**Figure 6.** Total annihilation rate  $\Gamma_\alpha$  with fixed  $m_\xi = 10$  GeV (left) and 100 GeV (right). Both plots are calculated with  $r_\rho = 1$ . Orange and blue lines are for  $\chi$  and  $\xi$  particles respectively. Solid line indicates  $\sigma_{\chi\xi} = 10^{-23} \text{ cm}^2$  and dot-dashed  $\sigma_{\chi\xi} = 10^{-24} \text{ cm}^2$ .  $\Gamma_\alpha$  with smaller  $n_\alpha$  is subject to a larger correction from the other specie. In the lower panel, the ratios between coupled and decoupled are shown. Purple shaded region indicates the evaporation region of  $\chi$ .

for a given DM specie  $\alpha$ . If it is in the equilibrium state, we can apply eqs. (5.1a) and (5.1b) and obtain

$$\Gamma_\chi^{\text{eq}} = \frac{1}{2} \frac{(C_s^\chi)^2}{C_a^\chi} \left( \frac{1}{2} + \sqrt{\frac{1}{4} + R_\chi} \right)^2, \quad (5.3a)$$

$$\Gamma_\xi^{\text{eq}} = \frac{1}{2} \frac{(C_s^\xi)^2}{C_a^\xi} \left( \frac{1}{2} + \sqrt{\frac{1}{4} + R_\xi} \right)^2, \quad (5.3b)$$

where  $R_{\chi,\xi}$  is given in eq. (5.1c). The above equations assume  $\xi$  dominates the DM population over  $\chi$ . Counter case is vice versa.

For a more general discussion, unless specified, we will not assume which specie is dominant over the other. The plot of  $\Gamma_\chi$  versus  $m_\chi$  is shown in figure 6 with  $r_\rho = 1$ . In this figure, we fixed  $m_\xi = 10$  GeV and 100 GeV while  $m_\chi$  runs from 1 GeV to 1000 GeV. In the above choice of parameters, both DM species are all in equilibrium state today. As a consequence of large interactions in the DS, the number of DM in the equilibrium state is affected little from the DM-nucleus interaction. Results from SI and SD cases are both similar. Therefore, we focus on the SI case only in the following discussion. In figure 6, the lower panel shows the ratio between coupled and decoupled cases. Such ratio indicates how strong is the correction from  $\sigma_{\chi\xi}$ .

On the left panel of figure 6, we fixed  $m_\xi = 10$  GeV and  $\Gamma_\xi$  is indicated by the blue line. When  $m_\chi > m_\xi$ , it is true that  $n_\chi < n_\xi$ . Hence  $\xi$  is the dominant specie in the

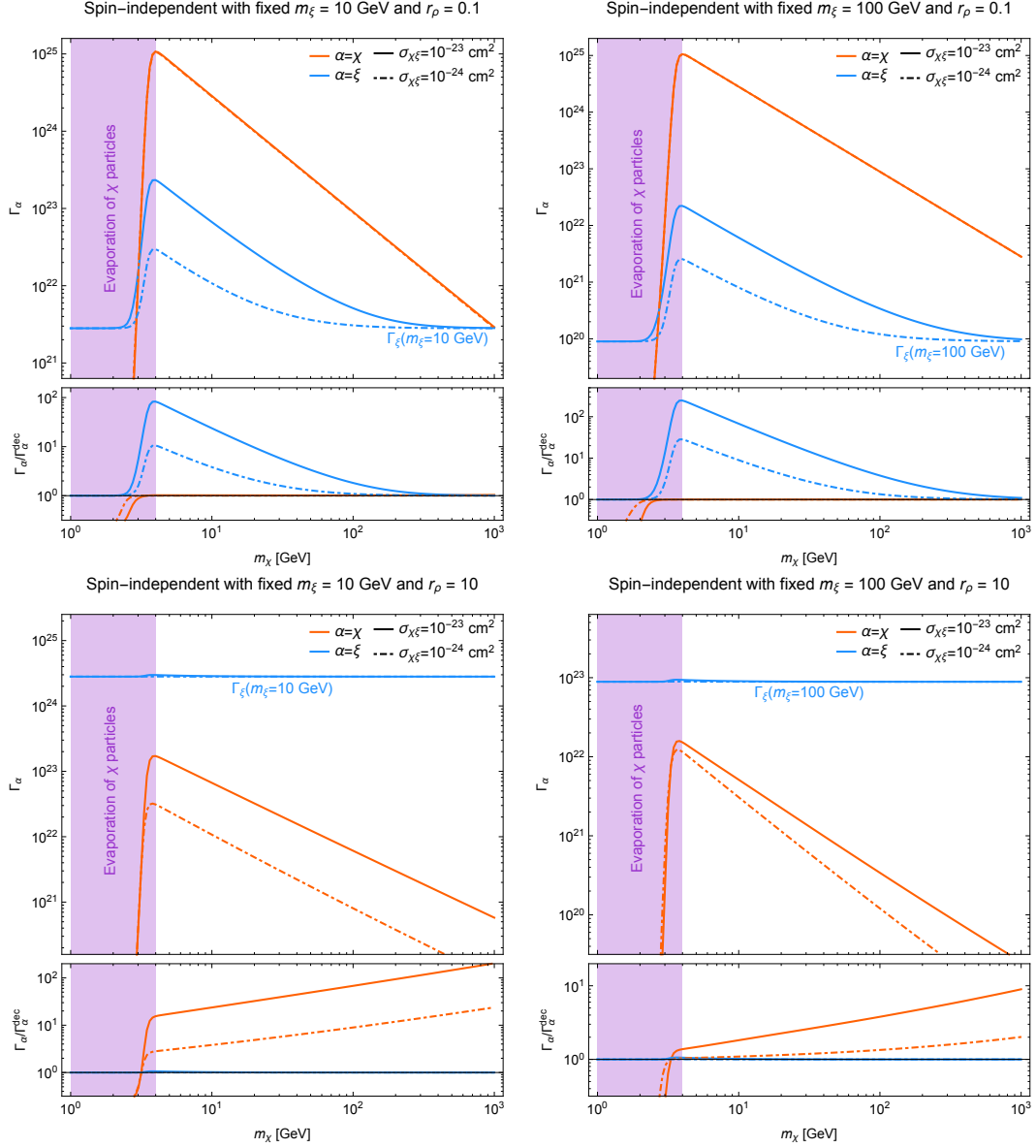


**Figure 7.** The same as figure 6 but  $r_\rho = 0.1$  (upper) and 10 (lower).

Sun and  $\Gamma_\xi$  can be considered as independent of  $\chi$  particles. But  $\Gamma_\chi$  is usually subject to a correction from  $\xi$  when  $m_\chi > m_\xi$ . However, when  $m_\chi$  is close to  $m_\xi$ , both numbers  $N_{\chi,\xi}$  are nearly equivalent. Mutual influence is strong in this region. Not only  $\Gamma_\chi$  is enhanced by  $\xi$  particles, as well as  $\Gamma_\xi$  is increased by  $\chi$  particles in the Sun. The ratio of correction is shown in the lower panel. A quick drop of  $\Gamma_\chi$  when  $m_\chi \lesssim 4$  GeV is due to the evaporation effect. The discussion is similar to the right figure of figure 6, instead of raising  $m_\xi$  to 100 GeV. Again, the correction from  $\xi$  to  $\Gamma_\chi$  is not significant when  $m_\chi > m_\xi$  here. Nonetheless, in the range  $m_\chi$  is smaller than  $m_\xi$  ( $n_\chi > n_\xi$ ),  $\Gamma_\xi$  is subject to a correction from  $\chi$ . Note that  $m_\chi = 100$  GeV ( $m_\xi = 10$  GeV) of the left figure is the same as the

right figure of  $m_\chi = 10 \text{ GeV}$  ( $m_\xi = 100 \text{ GeV}$ ). It can be realized from the symmetry of the evolution equations given in eqs. (3.5a) and (3.5b).

The case for  $r_\rho \neq 1$  is shown in figure 7. Parameters are the same as in the case of  $r_\rho = 1$  and the DM particles are also in the equilibrium state. We know that  $\Gamma_\alpha \propto C_s^2/C_a = n^2/\langle\sigma v\rangle$  and the ratio  $\Gamma_\chi/\Gamma_\xi \propto (m_\xi/m_\chi)^2/r_\rho^3$  in terms of eq. (2.7). Hence we can deduce that  $\Gamma_\chi/\Gamma_\xi \sim 1$  when  $m_\chi \approx 32m_\xi$  for  $r_\rho = 0.1$ . This statement is partially correct since the exact  $\Gamma_\alpha$  is subject to an extra correction factor from  $R_\alpha$  in eqs. (5.3a) and (5.3b). We have numerically verified the correction factor is roughly 3. Precisely speaking, when  $m_\chi \approx 100m_\xi$ ,  $\Gamma_\chi/\Gamma_\xi \sim 1$ . From the upper panel left in figure 7, it is clearly seen that  $\Gamma_\chi/\Gamma_\xi \sim 1$  when  $m_\chi \sim 1000 \text{ GeV}$ . This argument agrees with our numerical result well. Similarly, it applies to the case of  $m_\xi = 100 \text{ GeV}$ . In this case,  $\Gamma_\chi/\Gamma_\xi \sim 1$  when  $m_\chi \approx 10^4 \text{ GeV}$ . For  $r_\rho = 10$ , we can use the approximation above and obtain that  $\Gamma_\chi/\Gamma_\xi \sim 1$  when  $m_\chi \approx 0.01m_\xi$ . Therefore,  $m_\chi = 0.1(1) \text{ GeV}$  when  $m_\xi = 10(100) \text{ GeV}$  that we would have  $\Gamma_\chi/\Gamma_\xi \sim 1$ . However, one should bear in mind that for  $m_\chi \lesssim 4 \text{ GeV}$  all  $\chi$  particles have evaporated already.

## 6 Summary

In this paper, we address the issue of 2DM evolution in the Sun. We consider a scenario, where the heterogeneous  $\chi\xi$  self-scattering happens. Such interaction weaves the evolution processes for both DM species that was assumed to evolve independently. We found that when one DM specie is sub-dominant, its number of particles in the Sun is subject to a correction from the dominant specie. This correction always enhances the number of DM particles being captured. When the masses of the two DM species are close, the enhancement is mutual and has the largest impact. However, the sub-dominant specie in general has smaller total annihilation rate, the effect of heterogeneous self-capture would be tiny to the detection unless its annihilation final state is distinct from the dominant one.

Though the heterogeneous self-interaction causes extra self-evaporation and self-ejection, we have demonstrated that these negative effects are either small or it must happens when the DM mass is sufficient light,  $m_\alpha^{\text{ev}} \lesssim 4 \text{ GeV}$ . Therefore, in most of the interested mass range that relates to our study, they can be safely ignored.

To summarize, we would like to point out that the heterogeneous self-interaction is a natural consequence of any 2DM or  $n$ DM models. This effect will eventually reflect in the DM annihilation rates. Potentially, if the DM annihilates to the SM particles in the final state, such signal could be detected in the terrestrial detectors. Therefore, the strength of the heterogeneous self-interaction could be probed. Moreover, any sign of such interaction could be considered as a possible existence of DM beyond one-component.

## Acknowledgments

C. S. Chen (TKU) and Y. H. Lin (NCKU) are supported by the Ministry of Science and Technology, Taiwan under Grant No. 104-2112-M-032-009-MY3 and 106-2811-M-006-041



respectively.

## A Derivations of the 2DM heterogeneous self-scattering rates

### A.1 The self-capture rate

To the capture rate of different classes of particles has been fully discussed in refs. [47, 48, 68]. In this appendix, we only present the mathematical key point to derive the heterogeneous self-capture rate.

Following earlier works [48, 68], the problem begins by considering capture in a spherical shell of material (solar interior) on which capture is happening of radius  $r$  and local escape velocity  $v_{\text{esc}}(r)$ . Now at an imaginary surface bounding a region of radius  $R$ , which the solar gravity is negligible at  $R$ . The DM flux goes inward across the surface is [81]

$$\pi R^2 f(u) u du \frac{dJ^2}{R^2 u^2} \quad (\text{A.1})$$

where  $f(u)$  is the DM velocity distribution at infinity,  $J = Ru \sin \theta$  the angular momentum per unit mass and  $\theta$  the angle relative to the radial direction. Taking  $\Omega(w)$  is the rate at which a DM particle enters the shell  $r$  with velocity  $w = \sqrt{v_{\text{esc}}^2(r) + u^2}$  and scatters to velocity less than  $v_{\text{esc}}(r)$ . The probability of such a DM to be captured is [68]

$$dP = \frac{\Omega(w)}{w} \frac{2dr}{\sqrt{1 - J^2/(rw)^2}} \Theta(rw - J) \quad (\text{A.2})$$

where  $\Theta$  is the Heaviside step function. The differential rate of capture can be easily obtained by multiplying eqs. (A.1) and (A.2) then integrate over all angular momentum  $J^2$ . Replacing  $dV = 4\pi r^2 dr$  we have,

$$\frac{dC}{dV du} = \frac{f(u)}{u} w \Omega(w). \quad (\text{A.3})$$

Thus, the total DM capture rate per unit shell volume is given by

$$\frac{dC}{dV} = \int \frac{f(u)}{u} w \Omega(w) du. \quad (\text{A.4})$$

In the above equation,  $w$  depends on  $u$  explicitly. The remaining task is to determine  $\Omega(w)$ .

The scattering in the shell is simply  $n\sigma w$ , with the the scattering cross section  $\sigma$  and the target number density  $n$ . Practically we assume nearly isotropic and velocity-independent  $\sigma$ . The incoming particle with  $m_\chi$  and scatters off bounded particle with  $m_\xi$ . In order to be captured,  $\chi$  particle must loses a fractional of kinetic energy over the interval

$$\frac{u^2}{w^2} \leq \frac{\Delta E}{E} \leq \frac{\mu}{\mu_+^2} \quad (\text{A.5})$$

where  $\mu$  and  $\mu_\pm$  are expressed as

$$\mu = \frac{m_\chi}{m_\xi}, \quad \mu_\pm = \frac{\mu \pm 1}{2}, \quad (\text{A.6})$$

and  $\eta^2 = 3(v_\odot/\bar{v})^2/2$ ,  $v_\odot = 220 \text{ km s}^{-1}$  the solar moving velocity and  $\bar{v} = 270 \text{ km s}^{-1}$  the DM velocity dispersion.

Therefore, the capture probability in each scattering is

$$p_{\text{cap}} = \frac{\mu_+^2}{\mu} \left( \frac{\mu}{\mu_+^2} - \frac{u^2}{w^2} \right) \Theta \left( \frac{\mu}{\mu_+^2} - \frac{u^2}{w^2} \right). \quad (\text{A.7})$$

The rate of capture is simply the scattering rate  $n_\xi \sigma w$  times the capture probability  $p_{\text{cap}}$ . Hence,

$$\Omega(w) = n_\xi \sigma w p_{\text{cap}} = \frac{\sigma n_\xi v_{\text{esc}}^2(r)}{w} \left[ 1 - \frac{u^2}{v_{\text{esc}}^2(r)} \frac{\mu_-^2}{\mu} \right] \Theta \left( 1 - \frac{u^2}{v_{\text{esc}}^2(r)} \frac{\mu_-^2}{\mu} \right). \quad (\text{A.8})$$

Combining eqs. (A.4) and (A.8) we have

$$\frac{dC_s^{\chi \rightarrow \xi}}{dV} = \int \sigma n_\xi(r) v_{\text{esc}}^2(r) \frac{f(u)}{u} \left( 1 - \frac{u^2}{v_{\text{esc}}^2(r)} \frac{\mu_-^2}{\mu} \right) \Theta(v_{\text{esc}}^2(r) - \mu u^2) \quad (\text{A.9})$$

With respect to the solar moving frame, we can express  $f(u)$  as

$$f(u) = \frac{4}{\sqrt{\pi}} n_\chi x^2 e^{-x^2} e^{-\eta^2} \frac{\sinh(2x\eta)}{2x\eta} \quad (\text{A.10})$$

in terms of the dimensionless variables  $x^2 = 3(u/\bar{v})^2/2$  and  $\eta^2 = 3(v_\odot/\bar{v})^2/2$ . Integrating eq. (A.9) over  $u$ , we have

$$\begin{aligned} \frac{dC_s^{\chi \rightarrow \xi}}{dV} = & \sqrt{\frac{3}{2}} n_\chi n_\xi(r) \sigma_{\chi\xi} \frac{v_{\text{esc}}^2(r)}{2\eta\bar{v}Y^2} \left\{ \left( Y_+ Y_- - \frac{1}{2} \right) [X(-\eta, \eta) - X(Y_-, Y_+)] \right. \\ & \left. + \frac{1}{2} Y_+ e^{-Y_-^2} - \frac{1}{2} Y_- e^{-Y_+^2} - \eta e^{-\eta^2} \right\} \end{aligned} \quad (\text{A.11})$$

where we have replaced  $\sigma$  by  $\sigma_{\chi\xi}$  to indicate the heterogeneous self-scattering cross section and

$$Y^2 = \frac{3}{2} \frac{v_{\text{esc}}^2(r)}{\bar{v}^2} \frac{\mu}{\mu_-^2}, \quad Y_\pm = Y \pm \eta, \quad (\text{A.12a})$$

$$X(a, b) \equiv \int_a^b e^{-y^2} dy = \frac{\sqrt{\pi}}{2} [\text{erf}(b) - \text{erf}(a)]. \quad (\text{A.12b})$$

Thus, the coefficient of heterogeneous self-capture rate is evaluated as

$$C_s^{\chi \rightarrow \xi} = \frac{\int 4\pi r^2 (dC_s^{\chi \rightarrow \xi}/dV) dr}{\int 4\pi r^2 n_\xi(r) dr} \quad (\text{A.13})$$

where  $n_\xi(r)$  is the number distribution of  $\xi$  particles in the Sun. The case for halo  $\xi$  particle scatters with solar trapped  $\chi$  particle is essentially identical.

## A.2 The self-evaporation rate

Self-evaporation happens when two DM particles collide, one gets velocity larger than the escape velocity  $v_{\text{esc}}$ . Such calculation is similar to the evaporation between DM and nucleus presented in ref. [47]. Here we show the key to obtain the heterogeneous self-evaporation rate.

To scatter a  $\xi$  particle from velocity  $w$  to  $v_{\text{esc}} > w$  by  $\chi$  particle, the rate is

$$\begin{aligned} \Omega_{se}(w) = & \sqrt{\frac{2}{\pi}} \frac{T_\chi}{m_\xi} \frac{1}{\mu^2} \frac{\sigma_{\chi\xi} n_\chi(r)}{w} \left\{ \mu(\alpha_+ e^{-\alpha_-^2} - \alpha_- e^{-\alpha_+^2}) \right. \\ & + 2\mu_+^2 X(\beta_-, \beta_+) \exp \left[ -\frac{m_\xi}{2T_\chi} (v_{\text{esc}}^2(r) - w^2) \right] \\ & \left. + (\mu - 2\mu\alpha_+\alpha_- - 2\mu_+\mu_-) X(\alpha_-, \alpha_+) \right\} \end{aligned} \quad (\text{A.14})$$

where

$$\alpha_\pm = \sqrt{\frac{m_\chi}{T_\chi}} (\mu_+ v_{\text{esc}}(r) \pm \mu_- w), \quad (\text{A.15a})$$

$$\beta_\pm = \sqrt{\frac{m_\xi}{T_\xi}} (\mu_- v_{\text{esc}}(r) \pm \mu_+ w). \quad (\text{A.15b})$$

Assuming  $\xi$  particles are in a truncated Maxwell-Boltzmann distribution with a cutoff velocity  $w_c$ ,

$$f(w)dw = \frac{4}{\sqrt{\pi}} \left( \frac{m_\xi}{2T_\xi} \right)^{3/2} n_\xi(r) w^2 e^{-m_\xi w^2/(2T_\xi)} \Theta(w_c - w) dw. \quad (\text{A.16})$$

Thus,

$$\frac{dC_{se}^{\chi \rightarrow \xi}}{dV} = \int f(w) \Omega_{se}(w) dw \quad (\text{A.17})$$

In order to evaluate eq. (A.17), we assumed that  $T_\chi = T_\xi = T$  and  $w_c = v_{\text{esc}}$ .<sup>2</sup> Therefore,

$$\begin{aligned} \frac{dC_{se}^{\chi \rightarrow \xi}}{dV} = & \frac{2}{\pi} \sqrt{\frac{2T}{m_\xi}} n_\xi(r) n_\chi(r) \sigma_{\chi\xi} \left[ e^{-E_e/T} \left( -\beta_+ \beta_- - \frac{1}{2\mu} \right) X(\beta_-, \beta_+) \right. \\ & \left. + e^{-E_e/T} \left( \alpha_+ \alpha_- - \frac{1}{2\mu} \right) X(\alpha_-, \alpha_+) + e^{-(E_e/T + \alpha_+^2)} \sqrt{\frac{m_\chi}{2T}} v_{\text{esc}}(r) \right] \end{aligned} \quad (\text{A.18})$$

where  $E_e = m_\xi v_{\text{esc}}^2(r)/2$ . Therefore, we have the coefficient of the heterogeneous self-evaporation rate,

$$C_{se}^{\chi \rightarrow \xi} = \frac{\int 4\pi r^2 (dC_{se}^{\chi \rightarrow \xi}/dV) dr}{(\int 4\pi r^2 n_\chi(r) dr) (\int 4\pi r^2 n_\xi(r) dr)}. \quad (\text{A.19})$$

When  $m_\chi = m_\xi$ , it reduces to the 1DM case and a symmetric factor 1/2 should be introduced to avoid over counting.

---

<sup>2</sup>DM temperature could depend on its mass and in general  $T_\chi/T_\xi \neq 1$ . However, the deviation from unity is small [52].

### A.3 The self-ejection rate

Once the incoming  $\chi$  particle loses a fraction of energy  $\Delta E/E > v_{\text{esc}}^2(r)/w^2$  to a trapped particle  $\xi$ . The  $\xi$  particle will be ejected from the Sun. Following the derivation in the appendix A.1 but replacing  $p_{\text{cap}}$  by the ejection probability [68]

$$p_{\text{ejec}} = \frac{\mu_+^2}{\mu} \left( \frac{\mu}{\mu_+^2} - \frac{v_{\text{esc}}^2(r)}{w^2} \right) \Theta \left( \frac{\mu}{\mu_+^2} - \frac{v_{\text{esc}}^2(r)}{w^2} \right). \quad (\text{A.20})$$

Thus, the rate of ejection,

$$\Omega_{ej}(w) = \frac{n_\xi(r)\sigma_{\chi\xi}}{w} \left( u^2 - \frac{\mu_-^2}{\mu} v_{\text{esc}}^2(r) \right) \Theta \left( u^2 - \frac{\mu_-^2}{\mu} v_{\text{esc}}^2(r) \right). \quad (\text{A.21})$$

Integrating over the  $\chi$  number distribution in the halo  $f(u)$  given in eq. (A.10) we have

$$\frac{dC_{ej}^{\chi \rightarrow \xi}}{dV} = \int \sigma_{\chi\xi} n_\xi(r) \frac{f(u)}{u} \left( u^2 - \frac{\mu_-^2}{\mu} v_{\text{esc}}^2(r) \right) \Theta \left( u^2 - \frac{\mu_-^2}{\mu} v_{\text{esc}}^2(r) \right) du. \quad (\text{A.22})$$

By changing of variable we get

$$\frac{dC_{ej}^{\chi \rightarrow \xi}}{dV} = \int \frac{\sigma_{\chi\xi} n_\xi(r)}{K^2} \frac{\mu_-^2}{\mu} v_{\text{esc}}^2(r) \frac{f(x)}{x} (x^2 - K^2) \Theta(x - K) dx$$

where

$$K^2 = \frac{3}{2} \frac{v_{\text{esc}}^2(r)}{\bar{v}^2} \frac{\mu_-^2}{\mu} \quad \text{and} \quad K_\pm = K \pm \eta.$$

Therefore,

$$\begin{aligned} \frac{dC_{ej}^{\chi \rightarrow \xi}}{dV} &= \frac{4}{\sqrt{\pi}} \sigma_{\chi\xi} n_\chi n_\xi(r) \frac{\bar{v}}{3\eta} \left[ e^{-K_+^2} (e^{4K\eta} K_+ - K_-) \right. \\ &\quad \left. - \frac{1}{2} \left( K_+ K_- - \frac{1}{2} \right) X(K_-, K_+) \right]. \end{aligned} \quad (\text{A.23})$$

Our final result of the heterogeneous self-ejection rate is evaluated as

$$C_{ej}^{\chi \rightarrow \xi} = \frac{\int 4\pi r^2 (C_{ej}^{\chi \rightarrow \xi}/dV) dr}{\int 4\pi r^2 n_\xi(r) dr}. \quad (\text{A.24})$$

However, due to the large escape velocity in the Sun, such self-ejection effect is always insignificant comparing to other effects. Thus, we can safely ignore this correction in the DM evolution.

## References

- [1] G. Aad et al. [ATLAS Collaboration], *Search for new phenomena in final states with an energetic jet and large missing transverse momentum in pp collisions at  $\sqrt{s} = 8$  TeV with the ATLAS detector*, *Eur. Phys. J. C* **75**, 299 (2015) [Erratum *ibid* **75**, 408 (2015)] [arXiv:1502.01518 [hep-ex]].

- [2] J. Abdallah et al., *Simplified Models for Dark Matter Searches at the LHC*, *Phys. Dark Univ.* **9-10**, 8 (2015) [arXiv:1506.03116 [hep-ph]].
- [3] D. S. Akerib et al. [LUX Collaboration], *Results from a search for dark matter in the complete LUX exposure*, *Phys. Rev. Lett.* **118**, 021303 (2017) [arXiv:1608.07648 [astro-ph.CO]].
- [4] C. Amole et al. [PICO Collaboration], *Dark Matter Search Results from the PICO-60 C<sub>3</sub>F<sub>8</sub> Bubble Chamber*, *Phys. Rev. Lett.* **118**, 251301 (2017) [arXiv:1702.07666 [astro-ph.CO]].
- [5] D. S. Akerib et al. [LUX Collaboration], *Limits on spin-dependent WIMP-nucleon cross section obtained from the complete LUX exposure*, *Phys. Rev. Lett.* **118**, 251302 (2017) [arXiv:1705.03380 [astro-ph.CO]].
- [6] E. Aprile et al. [XENON Collaboration], *Search for WIMP Inelastic Scattering off Xenon Nuclei with XENON100*, *Phys. Rev. D* **96**, 022008 (2017) [arXiv:1705.05830 [hep-ex]].
- [7] M. G. Aartsen et al. [IceCube PINGU Collaboration], *Letter of Intent: The Precision IceCube Next Generation Upgrade (PINGU)*, arXiv:1401.2046 [physics.ins-det].
- [8] K. Choi et al. [Super-Kamiokande Collaboration], *Search for neutrinos from annihilation of captured low-mass dark matter particles in the Sun by Super-Kamiokande*, *Phys. Rev. Lett.* **114**, 141301 (2015) [arXiv:1503.04858 [hep-ex]].
- [9] M. G. Aartsen et al. [IceCube Collaboration], *Search for annihilating dark matter in the Sun with 3 years of IceCube data*, *Eur. Phys. J. C* **77**, 146 (2017) [arXiv:1612.05949 [astro-ph.HE]].
- [10] M. Aguilar et al. [AMS Collaboration], *Precision Measurement of the Helium Flux in Primary Cosmic Rays of Rigidities 1.9 GV to 3 TV with the Alpha Magnetic Spectrometer on the International Space Station*, *Phys. Rev. Lett.* **115**, 211101 (2015).
- [11] M. Ackermann et al. [Fermi-LAT Collaboration], *The Fermi Galactic Center GeV Excess and Implications for Dark Matter*, *Astrophys. J.* **840**, 43 (2017) [arXiv:1704.03910 [astro-ph.HE]].
- [12] G. Ambrosi et al. [DAMPE Collaboration], *Direct detection of a break in the teraelectronvolt cosmic-ray spectrum of electrons and positrons*, *Nature* **552**, 63 (2017) [arXiv:1711.10981 [astro-ph.HE]].
- [13] P. A. R. Ade et al. [Planck Collaboration], *Planck 2013 results. XVI. Cosmological parameters*, *Astron. Astrophys.* **571**, A16 (2014) [arXiv:1303.5076 [astro-ph.CO]].
- [14] T. Hambye, *JHEP* **0901**, 028 (2009) [arXiv:0811.0172 [hep-ph]].
- [15] O. Lebedev, H. M. Lee and Y. Mambrini, *Vector Higgs-portal dark matter and the invisible Higgs*, *Phys. Lett. B* **707**, 570 (2012) [arXiv:1111.4482 [hep-ph]].
- [16] K. Agashe, Y. Cui, L. Necib and J. Thaler, *(In)direct Detection of Boosted Dark Matter*, *JCAP* **1410**, 062 (2014) [arXiv:1405.7370 [hep-ph]].
- [17] C. Gross, O. Lebedev and Y. Mambrini, *Non-Abelian gauge fields as dark matter*, *JHEP* **1508**, 158 (2015) [arXiv:1505.07480 [hep-ph]].
- [18] G. Arcadi, C. Gross, O. Lebedev, Y. Mambrini, S. Pokorski and T. Toma, *Multicomponent Dark Matter from Gauge Symmetry*, *JHEP* **1612**, 081 (2016) [arXiv:1611.00365 [hep-ph]].
- [19] M. Aoki and T. Toma, *Implications of Two-component Dark Matter Induced by Forbidden Channels and Thermal Freeze-out*, *JCAP* **1701**, 042 (2017) [arXiv:1611.06746 [hep-ph]].

- [20] H. Alhazmi, K. Kong, G. Mohlabeng and J. C. Park, *Boosted Dark Matter at the Deep Underground Neutrino Experiment*, *JHEP* **1704**, 158 (2017) [arXiv:1611.09866 [hep-ph]].
- [21] A. Bhattacharya, R. Gandhi, A. Gupta and S. Mukhopadhyay, *Boosted Dark Matter and its implications for the features in IceCube HESE data*, *JCAP* **1705**, 002 (2017) [arXiv:1612.02834 [hep-ph]].
- [22] J. Herrero-Garcia, A. Scaffidi, M. White and A. G. Williams, *On the direct detection of multi-component dark matter: sensitivity studies and parameter estimation*, *JCAP* **1711**, 021 (2017) [arXiv:1709.01945 [hep-ph]].
- [23] M. V. Medvedev, *Cosmological Simulations of Multicomponent Cold Dark Matter*, *Phys. Rev. Lett.* **113**, 071303 (2014) [arXiv:1305.1307 [astro-ph.CO]].
- [24] D. N. Spergel and P. J. Steinhardt, *Observational evidence for selfinteracting cold dark matter*, *Phys. Rev. Lett.* **84**, 3760 (2000) [astro-ph/9909386].
- [25] R. Massey et al., *The behaviour of dark matter associated with four bright cluster galaxies in the 10 kpc core of Abell 3827*, *Mon. Not. Roy. Astron. Soc.* **449**, 3393 (2015) [arXiv:1504.03388 [astro-ph.CO]].
- [26] F. Kahlhoefer, K. Schmidt-Hoberg, J. Kummer and S. Sarkar, *On the interpretation of dark matter self-interactions in Abell 3827*, *Mon. Not. Roy. Astron. Soc.* **452**, L54 (2015) [arXiv:1504.06576 [astro-ph.CO]].
- [27] M. R. Buckley and P. J. Fox, *Dark Matter Self-Interactions and Light Force Carriers*, *Phys. Rev. D* **81**, 083522 (2010) [arXiv:0911.3898 [hep-ph]].
- [28] L. G. van den Aarssen, T. Bringmann and C. Pfrommer, *Is dark matter with long-range interactions a solution to all small-scale problems of  $\Lambda$  CDM cosmology?*, *Phys. Rev. Lett.* **109**, 231301 (2012) [arXiv:1205.5809 [astro-ph.CO]].
- [29] S. Tulin, H. B. Yu and K. M. Zurek, *Resonant Dark Forces and Small Scale Structure*, *Phys. Rev. Lett.* **110**, 111301 (2013) [arXiv:1210.0900 [hep-ph]].
- [30] J. F. Navarro, C. S. Frenk and S. D. M. White, *A Universal density profile from hierarchical clustering*, *Astrophys. J.* **490**, 493 (1997) [astro-ph/9611107].
- [31] B. Moore, *Evidence against dissipationless dark matter from observations of galaxy haloes*, *Nature* **370**, 629 (1994).
- [32] R. A. Flores and J. R. Primack, *Observational and theoretical constraints on singular dark matter halos*, *Astrophys. J.* **427**, L1 (1994) [astro-ph/9402004].
- [33] S. W. Randall, M. Markevitch, D. Clowe, A. H. Gonzalez and M. Bradac, *Constraints on the Self-Interaction Cross-Section of Dark Matter from Numerical Simulations of the Merging Galaxy Cluster 1E 0657-56*, *Astrophys. J.* **679**, 1173 (2008) [arXiv:0704.0261 [astro-ph]].
- [34] J. L. Feng, M. Kaplinghat and H. B. Yu, *Halo Shape and Relic Density Exclusions of Sommerfeld-Enhanced Dark Matter Explanations of Cosmic Ray Excesses*, *Phys. Rev. Lett.* **104**, 151301 (2010) [arXiv:0911.0422 [hep-ph]].
- [35] M. G. Walker and J. Penarrubia, *A Method for Measuring (Slopes of) the Mass Profiles of Dwarf Spheroidal Galaxies*, *Astrophys. J.* **742**, 20 (2011) [arXiv:1108.2404 [astro-ph.CO]].
- [36] M. G. Walker, *Dark Matter in the Milky Way's Dwarf Spheroidal Satellites*, arXiv:1205.0311[astro-ph.CO].

- [37] M. Boylan-Kolchin, J. S. Bullock and M. Kaplinghat, *Too big to fail? The puzzling darkness of massive Milky Way subhaloes*, *Mon. Not. Roy. Astron. Soc.* **415**, L40 (2011) [arXiv:1103.0007 [astro-ph.CO]]
- [38] M. Boylan-Kolchin, J. S. Bullock and M. Kaplinghat, *The Milky Way's bright satellites as an apparent failure of  $\Lambda$ CDM*, *Mon. Not. Roy. Astron. Soc.* **422**, 1203 (2012) [arXiv:1111.2048 [astro-ph.CO]].
- [39] O. D. Elbert, J. S. Bullock, S. Garrison-Kimmel, M. Rocha, J. Oorbe and A. H. G. Peter, *Core formation in dwarf haloes with self-interacting dark matter: no fine-tuning necessary*, *Mon. Not. Roy. Astron. Soc.* **453**, 29 (2015) [arXiv:1412.1477 [astro-ph.GA]].
- [40] K. A. Oman et al., *The unexpected diversity of dwarf galaxy rotation curves*, *Mon. Not. Roy. Astron. Soc.* **452**, 3650 (2015) [arXiv:1504.01437 [astro-ph.GA]].
- [41] O. D. Elbert, J. S. Bullock, M. Kaplinghat, S. Garrison-Kimmel, A. S. Graus and M. Rocha, *A Testable Conspiracy: Simulating Baryonic Effects on Self-Interacting Dark Matter Halos*, arXiv:1609.08626 [astro-ph.GA].
- [42] A. Kamada, M. Kaplinghat, A. B. Pace and H. B. Yu, *How the Self-Interacting Dark Matter Model Explains the Diverse Galactic Rotation Curves*, *Phys. Rev. Lett.* **119**, 111102 (2017) [arXiv:1611.02716 [astro-ph.GA]].
- [43] P. Creasey, O. Sameie, L. V. Sales, H. B. Yu, M. Vogelsberger and J. Zavala, *Spreading out and staying sharp - creating diverse rotation curves via baryonic and self-interaction effects*, *Mon. Not. Roy. Astron. Soc.* **468**, 2283 (2017) [arXiv:1612.03903 [astro-ph.GA]].
- [44] M. Valli and H. B. Yu, *Dark matter self-interactions from the internal dynamics of dwarf spheroidals*, arXiv:1711.03502 [astro-ph.GA].
- [45] A. Robertson et al., *The diverse density profiles of galaxy clusters with self-interacting dark matter plus baryons*, arXiv:1711.09096 [astro-ph.CO].
- [46] K. Griest and D. Seckel, *Cosmic Asymmetry, Neutrinos and the Sun*, *Nucl. Phys. B* **283**, 681 (1987) [Erratum *ibid* **296**, 1034 (1988)].
- [47] A. Gould, *WIMP Distribution in and Evaporation From the Sun*, *Astrophys. J.* **321**, 560 (1987).
- [48] A. Gould, *Resonant Enhancements in WIMP Capture by the Earth*, *Astrophys. J.* **321**, 571 (1987).
- [49] N. Bernal, J. Martn-Albo and S. Palomares-Ruiz, *A novel way of constraining WIMPs annihilations in the Sun: MeV neutrinos*, *JCAP* **1308**, 011 (2013) [arXiv:1208.0834 [hep-ph]].
- [50] S. Baum, L. Visinelli, K. Freese and P. Stengel, *Dark matter capture, subdominant WIMPs, and neutrino observatories*, *Phys. Rev. D* **95**, 043007 (2017) [arXiv:1611.09665 [astro-ph.CO]].
- [51] N. Fornengo, A. Masiero, F. S. Queiroz and C. E. Yaguna, *On the Role of Neutrinos Telescopes in the Search for Dark Matter Annihilations in the Sun*, *JCAP* **1712**, 012 (2017) [arXiv:1710.02155 [hep-ph]].
- [52] R. Garani and S. Palomares-Ruiz, *Dark matter in the Sun: scattering off electrons vs nucleons*, *JCAP* **1705**, 007 (2017) [arXiv:1702.02768 [hep-ph]].

- [53] P. Binetruy, G. Girardi and P. Salati, *Constraints on a System of Two Neutral Fermions From Cosmology*, *Nucl. Phys. B* **237**, 285 (1984).
- [54] K. Griest and D. Seckel, *Three exceptions in the calculation of relic abundances*, *Phys. Rev. D* **43**, 3191 (1991).
- [55] G. Bertone, D. Hooper and J. Silk, *Particle dark matter: Evidence, candidates and constraints*, *Phys. Rept.* **405**, 279 (2005) [hep-ph/0404175].
- [56] M. Blennow and S. Clementz, *Asymmetric capture of Dirac dark matter by the Sun*, *JCAP* **1508**, 036 (2015) [arXiv:1504.05813 [hep-ph]].
- [57] M. Blennow, S. Clementz and J. Herrero-Garcia, *Pinning down inelastic dark matter in the Sun and in direct detection*, *JCAP* **1604**, 004 (2016) [arXiv:1512.03317 [hep-ph]].
- [58] L. M. Krauss and F. Wilczek, *Discrete Gauge Symmetry in Continuum Theories*, *Phys. Rev. Lett.* **62**, 1221 (1989).
- [59] M. B. Hindmarsh and T. W. B. Kibble, *Cosmic strings*, *Rept. Prog. Phys.* **58**, 477 (1995) [hep-ph/9411342].
- [60] B. Batell, *Dark Discrete Gauge Symmetries*, *Phys. Rev. D* **83**, 035006 (2011) [arXiv:1007.0045 [hep-ph]].
- [61] Y. Mambrini, *The  $ZZ'$  kinetic mixing in the light of the recent direct and indirect dark matter searches*, *JCAP* **1107**, 009 (2011) [arXiv:1104.4799 [hep-ph]].
- [62] S. Baek, P. Ko, W. I. Park and E. Senaha, *Higgs Portal Vector Dark Matter: Revisited*, *JHEP* **1305**, 036 (2013) [arXiv:1212.2131 [hep-ph]].
- [63] C. Arina, T. Hambye, A. Ibarra and C. Weniger, *Intense Gamma-Ray Lines from Hidden Vector Dark Matter Decay*, *JCAP* **1003**, 024 (2010) [arXiv:0912.4496 [hep-ph]].
- [64] P. Ko and Y. Tang, *Galactic center  $\gamma$ -ray excess in hidden sector DM models with dark gauge symmetries: local  $Z_3$  symmetry as an example*, *JCAP* **1501**, 023 (2015) [arXiv:1407.5492 [hep-ph]].
- [65] N. Bernal, X. Chu, C. Garcia-Cely, T. Hambye and B. Zaldivar, *Production Regimes for Self-Interacting Dark Matter*, *JCAP* **1603**, 018 (2016) [arXiv:1510.08063 [hep-ph]].
- [66] M. Duch, B. Grzadkowski and D. Huang, *Strongly self-interacting vector dark matter via freeze-in*, *JHEP* **1801**, 020 (2018) [arXiv:1710.00320 [hep-ph]].
- [67] M. Heikinheimo, T. Tenkanen and K. Tuominen, *Prospects for indirect detection of frozen-in dark matter*, *Phys. Rev. D* **97**, 063002 (2018) [arXiv:1801.03089 [hep-ph]].
- [68] A. R. Zentner, *High-Energy Neutrinos From Dark Matter Particle Self-Capture Within the Sun*, *Phys. Rev. D* **80**, 063501 (2009) [arXiv:0907.3448 [astro-ph.HE]].
- [69] A. Gould, *Evaporation of WIMPs with arbitrary cross-sections*, *Astrophys. J.* **356**, 302 (1990).
- [70] C. S. Chen, F. F. Lee, G. L. Lin and Y. H. Lin, *Probing Dark Matter Self-Interaction in the Sun with IceCube-PINGU*, *JCAP* **1410**, 049 (2014) [arXiv:1408.5471 [hep-ph]].
- [71] G. Jungman, M. Kamionkowski and K. Griest, *Supersymmetric dark matter*, *Phys. Rept.* **267**, 195 (1996) [hep-ph/9506380].
- [72] J. Engel and P. Vogel, *Spin dependent cross-sections of weakly interacting massive particles on nuclei*, *Phys. Rev. D* **40**, 3132 (1989).



- [73] J. R. Ellis and R. A. Flores, *Realistic Predictions for the Detection of Supersymmetric Dark Matter*, *Nucl. Phys. B* **307**, 883 (1988).
- [74] A. F. Pacheco and D. Strottman, *Nuclear Structure Corrections to Estimates of the Spin Dependent WIMP Nucleus Cross-section*, *Phys. Rev. D* **40**, 2131 (1989).
- [75] J. Engel, S. Pittel and P. Vogel, *Nuclear physics of dark matter detection*, *Int. J. Mod. Phys. E* **1**, 1 (1992).
- [76] P. C. Divari, T. S. Kosmas, J. D. Vergados and L. D. Skouras, *Shell model calculations for light supersymmetric particle scattering off light nuclei*, *Phys. Rev. C* **61**, 054612 (2000).
- [77] V. A. Bednyakov and F. Simkovic, *Nuclear spin structure in dark matter search: The Zero momentum transfer limit*, *Phys. Part. Nucl.* **36**, 131 (2005) [hep-ph/0406218].
- [78] K. Choi, C. Rott and Y. Itow, *Impact of the dark matter velocity distribution on capture rates in the Sun*, *JCAP* **1405**, 049 (2014) [arXiv:1312.0273 [astro-ph.HE]].
- [79] C. S. Chen, G. L. Lin and Y. H. Lin, *Thermal transport of the solar captured dark matter and its impact on the indirect dark matter search*, *Phys. Dark Univ.* **14**, 35 (2016) [arXiv:1508.05263 [hep-ph]].
- [80] G. Busoni, A. De Simone and W. C. Huang, *On the Minimum Dark Matter Mass Testable by Neutrinos from the Sun*, *JCAP* **1307**, 010 (2013) [arXiv:1305.1817 [hep-ph]].
- [81] W. H. Press and D. N. Spergel, *Capture by the sun of a galactic population of weakly interacting massive particles*, *Astrophys. J.* **296**, 679 (1985).